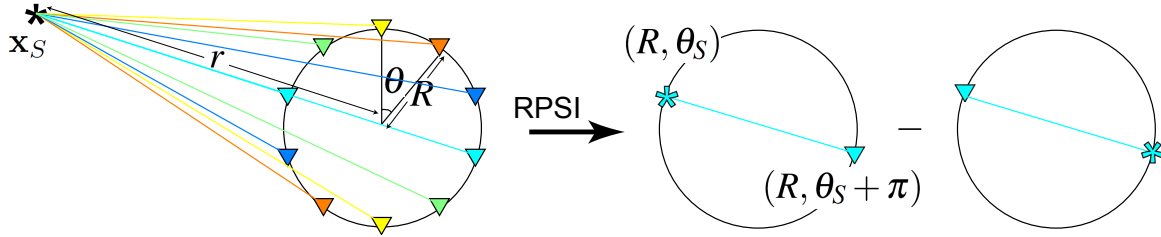


## Receiver-pair seismic interferometry and the cosine method

E.N. Ruigrok and K. Wapenaar

### Summary

In this paper we consider ambient seismicity with an a priori unknown, but strong, directionality. We develop methods to use the recorded Rayleigh waves for estimating an average dispersion curve and for estimating the directionality of the (noise) field. With the first method: receiver-pair seismic interferometry, a well-sampled circular array of receivers is used. The method consists of two steps. In the first step the recordings are crosscorrelated for opposite receiver pairs. From these crosscorrelations, the backazimuth of the source(s) are found with a stationary-phase analysis. In the second step, the crosscorrelations are stacked, yielding the actual surface-wave response between two positions on the circle. From the retrieved response, the dispersion curve is extracted. With the second method: the cosine method, there are only a few receivers on the circle. The backazimuth of the source is found from the crosscorrelations through an inversion scheme. A minimum of 4 receivers is required. Subsequently, we generalize the cosine method for non-circular arrays of receivers. For the generalized case a minimum of 3 receivers is required. In both latter cases, the dispersion curve can be found directly from the crosscorrelations after estimating the backazimuth of the source.



**Figure 1** A direct-wave configuration for receiver-pair seismic interferometry (RPSI). The response of a source (star at  $\mathbf{x}_S = (r, \theta_S)$ ) is measured with a circular array of receivers (coloured triangles) with radius  $R$ . After applying RPSI the response is obtained as if there were a source at location  $(R, \theta_S)$  and a receiver at  $(R, \theta_S + \pi)$  and vice versa.

## Introduction

The frequency dispersion of surface waves contains information about the seismic velocities as function of depth, allowing the estimation of velocity models (Knopoff, 1961). Initially, earthquake and controlled-source records were used to obtain dispersion curves that could subsequently be inverted for velocity profiles. Later, also a number of methods were developed to obtain the dispersion curves from noise recordings, e.g., by first applying seismic interferometry (Shapiro and Campillo, 2004) and with the SPAC method (Aki, 1965). With the latter two methods it is assumed that the noise comes from all directions. Especially for small recording times this is rarely the case. In this paper we consider the situation of a directionally strongly biased seismic (noise) field. We work out two new methods for estimating the backazimuth of the (noise) source(s) and extracting the dispersion curves from the recordings.

## Receiver-pair seismic interferometry (RPSI)

We use a cylindrical coordinate system with the origin located at the center of the circle (Fig. 1). The receivers are located on the edge of the circle with radius  $R$ . We consider wave propagation in the horizontal plane due to a vertical line source at  $\mathbf{x}_S = (r, \theta_S)$ . In the frequency domain, the impulse response at receiver location  $\mathbf{x} = (R, \theta)$  can be approximated as

$$u(\theta, \mathbf{x}_S, \omega) = 1/(\sqrt{8\pi k(r - R \cos(\theta - \theta_S))}) e^{-j(\omega(\frac{r}{v(f)} - \frac{R}{v(f)} \cos(\theta - \theta_S)) + \frac{\pi}{4})}, \quad (1)$$

where  $\frac{r}{v(f)} - \frac{R}{v(f)} \cos(\theta - \theta_S)$  is the frequency dependent traveltime. We omitted the radial coordinate for a receiver location. Similarly, the response recorded at  $\theta + \pi$  can be expressed as

$$u(\theta + \pi, \mathbf{x}_S, \omega) = 1/(\sqrt{8\pi k(r + R \cos(\theta - \theta_S))}) e^{-j(\omega(\frac{r}{v(f)} + \frac{R}{v(f)} \cos(\theta - \theta_S)) + \frac{\pi}{4})}. \quad (2)$$

Crosscorrelating equation 1 and 2 results in

$$u(\theta, \mathbf{x}_S, \omega)^* u(\theta + \pi, \mathbf{x}_S, \omega) = 1/(8\pi k \sqrt{r^2 + R^2 \cos^2(\theta - \theta_S)}) e^{-j(\omega(\frac{2R}{v(f)} \cos(\theta - \theta_S))}. \quad (3)$$

Integrating equation 3 over  $\theta$  and applying a stationary-phase approximation (Bleistein, 1984) yields

$$\frac{2j\omega}{v(f)} \oint_0^{2\pi} u(\theta, \mathbf{x}_S, \omega)^* u(\theta + \pi, \mathbf{x}_S, \omega) d\theta \propto u(\theta_S + \pi, \theta_S, \omega) - u(\theta_S, \theta_S + \pi, \omega)^*, \quad (4)$$

where  $*$  denotes complex conjugation. Note that in equation 4 the integration is over receiver pairs instead of over sources (e.g., Wapenaar (2004)) or receivers (e.g., Curtis et al. (2009)). Hence the name "receiver-pair seismic interferometry" (RPSI). As with other types of seismic interferometry, with RPSI a response is retrieved between two positions. These positions are located on the circle in Fig. 1 and do not necessarily correspond to actual receiver positions. An additional stationary-phase analysis is required to find the positions of the virtual source and the virtual receiver. There is a plane-wave approximation in equations 1 and 2. However, in the stationary-phase points ( $\theta = \theta_S$  &  $\theta = \theta_S + \pi$ ) equations 1 and 2 are also accurate for spherical waves.

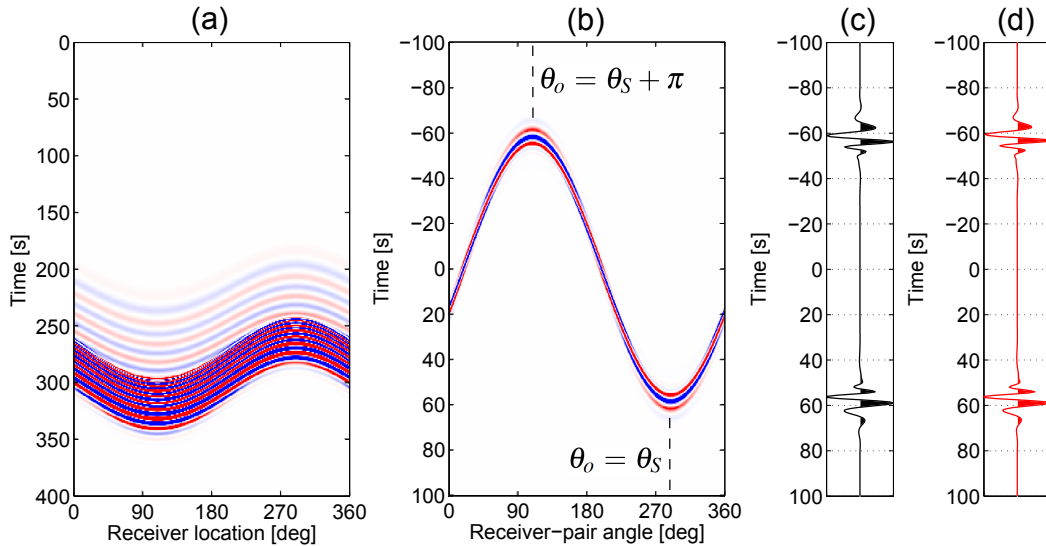


**Figure 2** (a) Rayleigh wave recordings for a single source and a circular array of receivers (similar to Fig. 1). (b) The integrand of equation 3 for the recordings in (a), with the stationary points ( $\theta_o$ ) marked. (c) The result of stacking (b) over receiver-pair angles. (d) The Rayleigh-wave response for a source at  $(R, \theta_S)$  and a receiver at  $(R, \theta_S + \pi)$  and minus this response time-reversed.

### Numerical illustration of RPSI

In the following we show a crustal-scale numerical example of RPSI with a single transient source. Note that this example can easily be scaled to an exploration-scale example. We use the configuration as in Fig. 1 with a low-frequency source at  $(r, \theta_S) = (800\text{km}, 290^\circ)$  and 720 receivers on the circle with a 80 km radius. The source wavelet is a Ricker function with a central frequency of 0.18 Hz. The fundamental-mode Rayleigh waves are forward modeled, using the dispersion curve as depicted with the dashed black line in Fig. 3(a). The dispersion curve is computed for the upper 300 km of a 1D Earth model. The resulting surface-wave recordings are shown in Fig. 2(a).

With RPSI (equation 4) the recording of each receiver is crosscorrelated with the recording at the receiver at the opposite site of the circle (Fig. 1). The crosscorrelation result as function of receiver-pair angle is shown in Fig. 2(b). This correlation function has two stationary points ( $dt/d\theta=0$ ). The stationary point  $\theta_o$  for which the correlation function is stationary at positive times is the backazimuth of the source  $\theta_S$ .

The last step of RPSI is stacking the crosscorrelations (Fig. 2b) over receiver-pair angles and taking the time derivative yielding Fig. 2(c). This trace is compared with Fig. 2(d), which is the forward modeled response for a source at  $(R, \theta_S)$  and a receiver at  $(R, \theta_S + \pi)$  and minus this response time-reversed. The latter two traces are nearly identical and thus confirm equation 4 numerically.

As a further verification we extract the dispersion curve  $v(f)$  from the causal retrieval. Fig. 3(a) shows the used dispersion curve for the forward modeling (black dashed line) and the extracted dispersion curve from the RPSI result (red dashed line). The effective spectrum of the RPSI result is shown in Fig. 3(b). It can be seen that the dispersion curve is well estimated for the frequency band in which there is sufficient amplitude.

### The cosine method

For a straightforward application of RPSI (see previous section) a well-sampled array of receivers is required. With only a few receivers on the circle (Fig. 1) the RPSI integral (equation 4) is not well approximated. Still,  $\theta_S$  and  $v(f)$  of the medium within the circle can be found. However, an inversion approach is required. In this section we will describe this approach.

From the crosscorrelation (equation 3) of a single wavetrain detected at two receivers with  $\pi$  rad separation, we find the traveltime difference:  $t^d(\theta, f) = \frac{2R}{v(f)}(\cos(\theta)\cos(\theta_S) + \sin(\theta)\sin(\theta_S))$ . Hence,

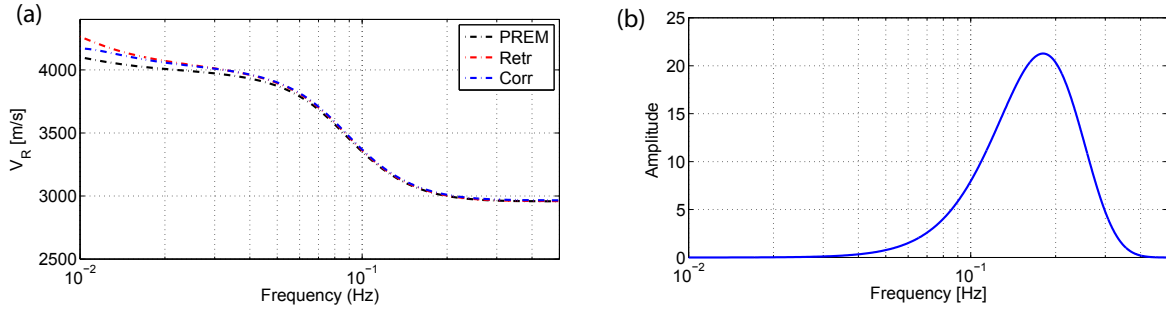


**Figure 3** (a) The actual (black line) and estimated (coloured lines) dispersion curves and (b) the amplitude spectrum of the source.

for  $n$  receivers the following system of equations can be composed:

$$\begin{bmatrix} 2R \cos(\theta_1) & 2R \sin(\theta_1) \\ 2R \cos(\theta_2) & 2R \sin(\theta_2) \\ \vdots & \vdots \\ 2R \cos(\theta_{n/2}) & 2R \sin(\theta_{n/2}) \end{bmatrix} \begin{bmatrix} \frac{1}{v(f)} \cos(\theta_S) \\ \frac{1}{v(f)} \sin(\theta_S) \end{bmatrix} = \begin{bmatrix} t^d(\theta_1, f) \\ t^d(\theta_2, f) \\ \vdots \\ t^d(\theta_{n/2}, f) \end{bmatrix} \quad (5)$$

where  $n/2$  is the number of receiver pairs.

The above system of equations is in the form  $\mathbf{Gm} = \mathbf{d}$ . Having two unknowns ( $\theta_S$  &  $v(f)$ ) this system can be solved for two or more receiver pairs ( $n \geq 4$ ).

We solve this system only once for the entire spectrum of the source (Fig. 3b). From the crosscorrelations we pick the arrival times of the peak energy, as an estimate of  $t^d(\theta_i)$ . Subsequently, we solve the system of equations by ordinary least squares (Aster et al., 2004):  $\mathbf{m} = (\mathbf{G}^T \mathbf{G})^{-1} \mathbf{G}^T \mathbf{d}$ , where  $T$  denotes the transpose and  $^{-1}$  denotes the inverse of a matrix.

From the recording in the previous section we select 4 out of the 720 receivers. We find the following values:  $t^d(0^\circ, f^c) = 19.65$  and  $t^d(90^\circ, f^c) = -54.70$  s. We solve the system of equations and find  $m_1 = 0.1228$  and  $m_2 = -0.3419$ . From the expressions for  $\mathbf{m}$  (equation 5) we subsequently isolate  $\theta_S$  finding an estimate of  $289.76^\circ$ , which is a tiny mismatch with respect to the actual value of  $290^\circ$ .

The dispersion curve is estimated from the crosscorrelations, which have the following phase term (equation 3):  $\phi(f) = -4\pi f R \cos(\theta_i - \theta_S) / v(f)$ . Hence, from a crosscorrelation the dispersion curve can be found with  $v(f) = -4\pi f R \cos(\theta_i - \theta_S) / \phi(f)$ . The estimation is least noise prone for the largest cosine term. Hence, knowing now the source backazimuth, we use the crosscorrelation for  $\theta = 270^\circ$ . Fig. 3(a) shows the extracted dispersion curve from the crosscorrelation with a dashed blue line. It can be seen that the dispersion curve is extracted as accurately as in the previous section.

The above inversion for  $\theta_S$  and  $v(f)$  are both based on the cosine phase expression of the crosscorrelation (equation 3). Hence the name "the cosine method".

### The generalized cosine method

Equation 5 still holds for receiver pairs with varying lengths. For receiver pairs with non-overlapping midpoints, however,  $\theta_S$  is not anymore uniquely defined. In this case we obtain the generalized cosine method by making the assumption that  $\theta_{Sij} = \theta_S$ , where  $i$  and  $j$  are the two receiver indexes defining a receiver pair.

Fig. 4(a) shows an arbitrary array with a nearby source. The origin of the coordinate system is chosen to be the centre of gravity of the receiver array.  $\theta_S$  is defined with respect to this centre and equals  $320^\circ$ . The configuration has 6 receivers ( $n=6$ ) and  $n(n-1)/2=15$  receiver pairs. In Fig. 4(a) the 15 connecting lines are drawn as well as their midpoints. For a receiver pair we define  $h_{ij}$  as the half offset.  $\theta_{ij}$  is the bearing of the interconnecting line with respect to Y-axis (North). For this configuration we find a new system of equations by replacing, in equation 5,  $R$  by  $h_{ij}$  and  $\theta_i$  by  $\theta_{ij}$ .

Fig. 4(b) shows 400 s from 8192 s of forward modeled noise. Fig. 4(c) is the result of crosscorrelating the recordings for each possible receiver pair and plotting the results as function of the receiver-pair

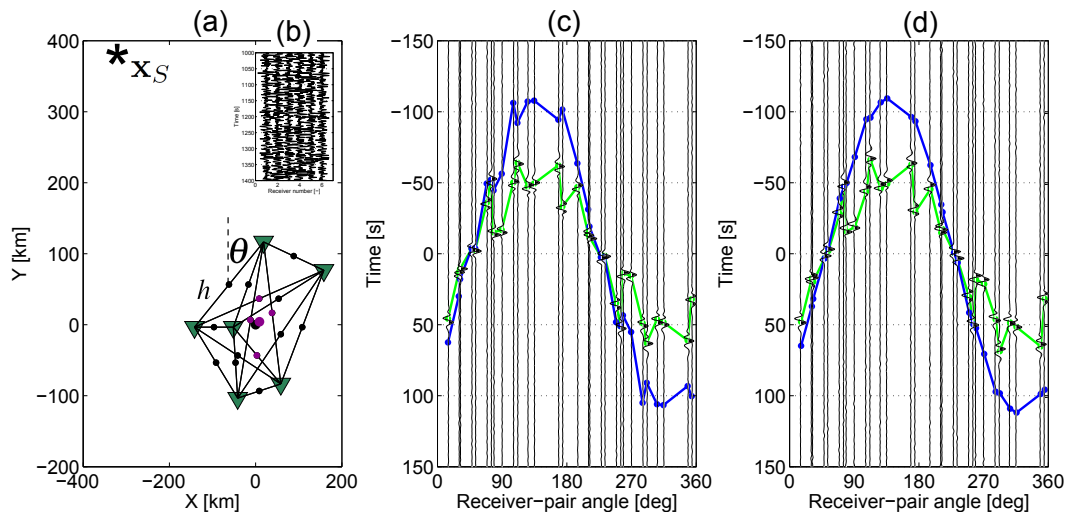


**Figure 4** (a) The response of a source (star at  $\mathbf{x}_S$ ) is measured with an array of receivers (green triangles). (b) 400 s of noise recorded at the 6 receivers. (c) The crosscorrelation of the noise recordings for all the possible pairs of receivers in (a), plotted as function of receiver-pair angle  $\theta$ . The plot is overlain by the picked timing of the crosscorrelations (green line) and the timing scaled by the receiver-pair distance  $h$  (blue line). (d) Same as (c) but for a source at 2000 km distance instead of 500 km.

angle. From Fig. 4(c)  $t^d(\theta_{ij}, f^c)$  is extracted. This timing is overlain in Fig. 4(d) as the green line. This function does not really look like a cosine due to the imprint of a varying  $h_{ij}$ . We restore a fixed receiver distance by multiplying  $t^d(\theta_{ij}, f^c)$  with  $\max(h_{ij})/h_{ij}$ , yielding the blue line.

Solving the system of equations and isolating  $\theta_S$  from the expressions for  $\mathbf{m}$  (equation 5) we estimate  $\theta_S$  to be  $317.21^\circ$ . This is an error of 0.78%. The error is mainly caused by the wide spread in midpoints and, as a result, the variation of  $\theta_{Sij}$ . Fig. 4(d) shows the picked time differences for a source with the same backazimuth, but located 4 times as far. For this configuration, the variation of  $\theta_{Sij}$  is smaller and the blue line thus better resembles a cosine. Consequently, the location error reduces to 0.21%. Alternatively, we can better satisfy the  $\theta_{Sij} = \theta_S$  assumption by only using receiver pairs with midpoints close to each other. We turn back to the configuration with the nearby source. Fig. 4(a) shows a subset of midpoints in purple. The big purple point is the new centre of gravity, for which  $\theta_S = 318.86^\circ$ . Using only the subset of receiver pairs, we estimate  $\theta_S$  to be  $318.04^\circ$ , which corresponds to an error of 0.23%. After estimating  $\theta_S$  the dispersion curve can be found again as in the previous section.

## Conclusions

In this paper we considered ambient seismicity with an a priori unknown directionality. We developed methods to use the recorded surface waves for estimating an average dispersion curve and for estimating the directionality of the (noise) field. Receiver-pair interferometry and the cosine method hold for both planar and spherical wavefronts. The generalized cosine method becomes increasingly inaccurate for nearby sources.

## References

- Aki, K. [1965] A note on the use of microseisms in determining the shallow structures of the Earth's crust. *Geophysics*, **30**, 665–666.
- Aster, R., Borchers, B. and Thurber, C. [2004] *Parameter estimation and inverse problems*, Academic Press.
- Bleistein, N. [1984] *Mathematical methods for wave phenomena*, Academic Press.
- Curtis, A., Nicolson, H., Halliday, D., Trampert, J. and Baptie, B. [2009] Virtual seismometers in the subsurface of the earth from seismic interferometry. *Nature Geoscience*, **2**, 700–704.
- Knopoff, L. [1961] Green's function for eigenvalue problems and the inversion of Love wave dispersion data. *Geophysical Journal International*, **4**, 161–173.
- Shapiro, N. and Campillo, M. [2004] Emergence of broadband Rayleigh waves from correlations of the ambient seismic noise. *Geophysical Research Letters*, **31**, doi:10.1029/2004GL019491.
- Wapenaar, K. [2004] Retrieving the elastodynamic Green's function of an arbitrary inhomogeneous medium by cross-correlation. *Physical Review Letters*, **93**, 254301–1–254301–4.